

Robot-Assisted Needle Alignment with Image-Guided Teleoperated Needle Insertion for Prostate Cancer Interventions

Gregory Scott Fischer¹, Weijian Shang¹, and Hao Su¹

¹Worcester Polytechnic Institute, Worcester, MA, United States

Introduction: In 2011, there are approximately 240,890 cases of prostate cancer in United States, with an estimated 1.2 million biopsies performed. Transrectal ultrasound (TRUS) guidance is the most commonly used navigation method for the prostate biopsy, however it has a poor cancer detection rate of 20% to 30 %, which is the main reason why more than 75% of biopsies are negative. The advantages of deploying a robotic system in prostate interventions include: 1) robot-assisted surgery guarantees good geometric accuracy overcoming the accuracy limits of traditional mechanical templates (5mm resolution), 2) robots can be designed with appropriate scale to fit into the center of a scanner bore, 3) teleoperation provides a better ergonomics than manual insertion which is awkward for physician to perform when the surgical sites are usually at the isocenter, and 4) real-time needle position information can be used to aid the surgical procedure. MR provides the ability to perform closed-loop image-guided surgery. However, the inability to use conventional sensors and actuators in high-field MR limits the availability of assistive technologies for interventional procedures. We have developed a modular MRI robot controller (Fig. 1) designed for operating all commonly used piezoelectric actuators, sensor and actuator modules for use in interventional MR devices, extensible software interfaces, and robotic surgery platforms for Neurosurgery and Prostate Interventions. The focus of this abstract is a robot developed to mimic the workflow of traditional template-guided prostate interventions where the robot aligns the needle path and a clinician controls insertion depth manually using a remote control from just outside the scanner bore.

Materials/Methods: A 6 degree of freedom (DOF) robot has been developed for performing prostate interventions inside the bore of 3T MRI. The robot, shown in Fig. 2 (right), provides for three axes of Cartesian positioning (2-DOF lateral alignment and 1-DOF placement of the robot tip against the perineum) and a 3-DOF needle driver module (needle insertion, cannula retraction or biopsy firing, and needle rotation). The needle insertion may be controlled automatically or by following the position of the teleoperation master device that the clinician operates as shown in Fig. 2 (left). Needle rotation may be turned on to assist in providing straighter insertion; parallel research efforts utilize needle rotation for active steering of a bevel tip needle's trajectory. The robot is actuated using PiezoLegs motors from Piezomotor and joint-level sensing is provided by optical encoders utilizing shielded differential signaling. The robot is controlled using a custom-developed robot control system that resides in the scanner room as shown in Fig. 1. The robot controller is fully self-contained and scanner-independent; the only connections are to the robot, a grounded AC socket in the scanner room, and fiber optic Ethernet to an external workstation. The fully shielded enclosure contains a linear AC-DC converter, low-frequency filtered DC-DC converters, an application-specific backplane, and the custom-developed control boards. Each board can perform closed loop position and velocity control of one non-resonant motor (e.g. Piezomotor) or a pair of resonant motors (e.g. Nanomotion, Shisei, PCB Motor) using an FPGA-based waveform synthesizer and low-noise filtered linear amplifiers. The robot may be controlled through a custom software interface, or 3D Slicer and any other OpenIGTLINK compliant application.

Experiments and Results: *MR Compatibility of the robotic system* was evaluated in a 3T Philips Achieva using four standard imaging protocols: T1-weighted fast gradient echo (T1 FGE/FFE), T2-weighted fast spin echo (T2 FSE/TSE), Real-time fast gradient echo (FGRE) and functional imaging spin echo-planar imaging (SE EPI). Results showing subtraction images and signal to noise (SNR) degradation are shown in Fig. 3. SNR was calculated as the mean signal in a 25pixel (~8mm) square ROI inside of the phantom divided by the RMS value of the noise in a 25pixel (~8mm) square ROI in the periphery of the image outside of the phantom and nearby ringing artifacts. SNR degradation proved to be visually unidentifiable and resulted in a mean SNR loss of 2.1% in the worst case. *Robot joint space accuracy* was assessed for the piezoelectrically actuated system. Resolution of the linear quadrature optical encoders integrated into the robot is 0.0127 mm/count (0.0005" resolution). A digital dial gauge with the same resolution is utilized for independent measurement, where both the robot and the dial gauge are rigidly mounted on a fixture table. Each linear axis of robot was commanded to move in 1 mm increments 40 times and the relative change in dial gauge reading recorded. In all cases, the control system maintained accuracy within one encoder count. Based on independent measurement (which includes deflection, misalignment, etc.), the joints can be reliably controlled to within 30 μ m. *Registration of the robot to the patient coordinate system* is based on imaging a fiducial frame attached to the robot, as shown in Fig. 2 (right), made of seven tubes filled with high contrast fluid and configured in a set of Z shapes. The registration algorithm segments the image and compensates for the irregular shape of the fiducial to find the best fitting ellipse. The seven points from several slices are utilized to calculate the 6-DOF position and orientation of the robot with respect to the scanner origin. An independent evaluation of registration accuracy in the MRI scanner showed sub-pixel resolution with a mean error of 0.27mm in translation and 0.16° in orientation; the corresponding RMS error is 0.33mm and 0.46°.

Discussion: Intraoperative MR imaging provides up-to-date anatomical information for ensuring that the surgical plan is properly executed. Further, real-time imaging can be used to visualize instrument tip and target location as the needle is inserted. The presented system provides a clinically viable approach to extending the standard workflow for template-guided, needle-based prostate interventions to take advantage of intraoperative MR imaging. Rather than requiring the clinician to reach inside the bore or translate the patient out (eliminating the possibility of live imaging), the teleoperated needle guide allows the physician to maintain control over needle insertion from inside the scanner room while leveraging the advantages of robotics and providing improved ergonomics. The robot can actively manipulate standard MR-compatible needles under live imaging aligned with the needle axis with negligible image quality degradation.

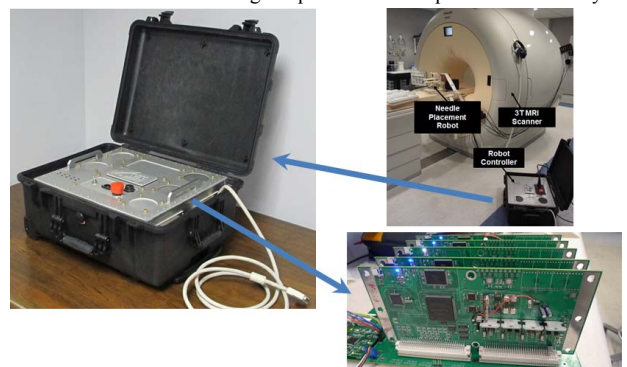


Figure 1: The MRI robot controller system – we developed a modular control system including a set of 4-ch low noise, high-power, waveform synthesizers that plug into an application-specific backplane that resides inside the shielded enclosure shown. The system can perform closed loop control of all commonly used commercially available piezoelectric actuators with no noticeable image quality degradation during simultaneous imaging and robot motion.

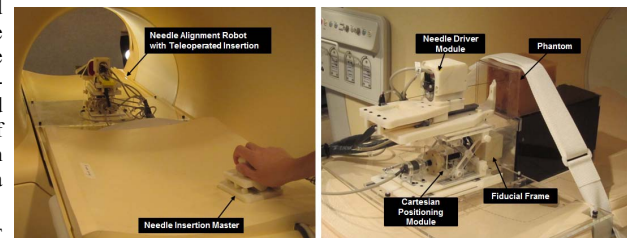


Figure 2: The robotic system developed for MR image-guided prostate biopsy and brachytherapy. The robot operates inside the bore during imaging, is registered to the scanner using a fiducial frame, and aligns the needle to targets selected in intraoperative MR imaging. The needle is inserted using a master device that lets the clinician stand beside the patient, view real-time MR images aligned with the needle axis, and control the needle depth while monitoring on the live images.

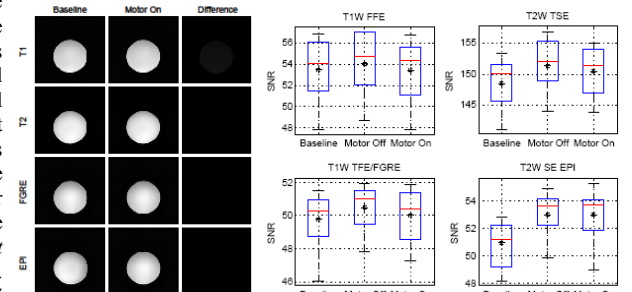


Figure 3: Results demonstrating the piezoelectric motors and custom drive circuits produce no statistically significant image degradation when the robot is moving during imaging. Qualitative results from representative images also demonstrate no distortion (left). Quantitative analysis of SNR for four imaging protocols with the robot absent, present but off, and actively moving (right). The SNR error is 0.33mm and 0.46°.